

# Search for a kaonic nuclear state via ${}^4\text{He}(K^-, N)$ reaction at rest

M. Iwasaki<sup>1,2</sup>, H. Bhang<sup>3</sup>, J. Chiba<sup>4</sup>, S. Choi<sup>3</sup>, Y. Fukuda<sup>2</sup>, T. Hanaki<sup>4</sup>, R. S. Hayano<sup>5</sup>, M. Iio<sup>1</sup>, T. Ishikawa<sup>5</sup>, S. Ishimoto<sup>6</sup>, T. Ishiwatari<sup>7</sup>, K. Itahashi<sup>1</sup>, M. Iwai<sup>6</sup>, P. Kienle<sup>7,8</sup>, J. H. Kim<sup>9</sup>, Y. Matsuda<sup>1</sup>, H. Ohnishi<sup>1</sup>, S. Okada<sup>1</sup>, H. Outa<sup>1</sup>, M. Sato<sup>1,2</sup>, S. Suzuki<sup>6</sup>, T. Suzuki<sup>1</sup>, D. Tomono<sup>1</sup>, E. Widmann<sup>7</sup>, T. Yamazaki<sup>1,5</sup>, and H. Yim<sup>3</sup>

<sup>1</sup> Nishina Center for Accelerator-Based Science, RIKEN

<sup>2</sup> Department of Physics, Tokyo Institute of Technology

<sup>3</sup> School of Physics, Seoul National University

<sup>4</sup> Department of Physics, Tokyo University of Science

<sup>5</sup> Department of Physics, University of Tokyo

<sup>6</sup> IPNS, KEK (High Energy Accelerator Research Organization)

<sup>7</sup> Stefan Meyer Institut für Subatomare Physik

<sup>8</sup> Physik Department, Technische Universität München

<sup>9</sup> Korea Research Institute of Standard and Science

Received: date / Revised version: date

**Abstract.** Very recently, we have performed a couple of experiments, *KEK PS-E549/E570*, for the detailed study of the strange tribaryon  $S^0(3115)$  obtained in *KEK PS-E471*. These experiments were performed to accumulate much higher statistics with improved experimental apparatus especially for the better proton spectroscopy of the  ${}^4\text{He}(\textit{stopped } K^-, N)$  reaction. In contrast to the previous proton spectrum, no narrow ( $\sim 20$  MeV) peak structure was found either in the inclusive  ${}^4\text{He}(\textit{stopped } K^-, p)$  or in the semi-inclusive  ${}^4\text{He}(\textit{stopped } K^-, pX^\pm)$  reaction channel, which is equivalent to the previous *E471* event trigger condition. Detailed analysis of the present data and simulation shows that the peak, corresponding to  $S^0(3115)$ , has been an experimental artifact. Present analysis does not exclude the possible existence of a much wider structure. To be sensitive to such structure and for better understanding of the non-mesonic  $K^-$  absorption reaction channel, detailed analysis of the data is in progress.

**PACS.** 13.75.Jz Kaon-baryon interaction

## 1 Introduction

Recently, the *KEK PS-E471* group reported the observation of peak formation in their *proton* spectrum, which corresponds to the formation of a three baryon system with strangeness  $-1$  and isospin  $1$  [1]. This experimental search was motivated by the theoretical prediction by Akaishi and Yamazaki [2], that the  $\bar{K}$  meson may form strong bound states by several light nuclei with an isospin zero. The most stable one is predicted to be formed by  $K^-$  with  ${}^3\text{He}$  core, so that the experimental search aiming at *neutron* spectroscopy was performed by using the  ${}^4\text{He}(\textit{stopped } K^-, n)$  reaction.

If one assumes that the peak corresponds to the kaonic nuclear bound state, then it means that the none-zero isospin state is formed with extremely large ( $\sim 200$  MeV) binding energy, while the predicted state has isospin zero with binding energy about 100 MeV. These are very outstanding features. If the assumption is true, the formed system could be more dense than the original theoretical prediction. Therefore, experimental confirmation is strongly required.

## 2 Upgraded Experimental Setup

We improved the experimental setup as shown in Figs. 1 and 2, based on the *E471* setup (given in reference [1]), to achieve confirmatory experiment shortly before KEK-PS shutdown. The previous *E471* setup was optimized to perform neutron spectroscopy by the time-of-flight (TOF) method from the (*stopped*  $K^-$ ,  $nX^\pm$ ) reaction on a liquid  ${}^4\text{He}$  target, where  $X^\pm$  is one of the decay charged particles detected by the top and bottom trigger counter system (TC). The neutron TOF can be calculated from the time difference between incoming kaon timing at T0 counters and one of the NC array, by subtracting kaon stopping time using its range information calculated from the vertex between  $K^-$  and  $X^\pm$  tracks.

The energy resolution and detection efficiency for neutrons was improved by replacing single-layered segmented kaon timing counters T0 with double-layered ones, and enlarging the number of neutron counter arrays (NC). For the neutron spectroscopy, the track information of this additional charged particle  $X^\pm$  on TC is indispensable even with the present setup to identify the kaon reaction point.

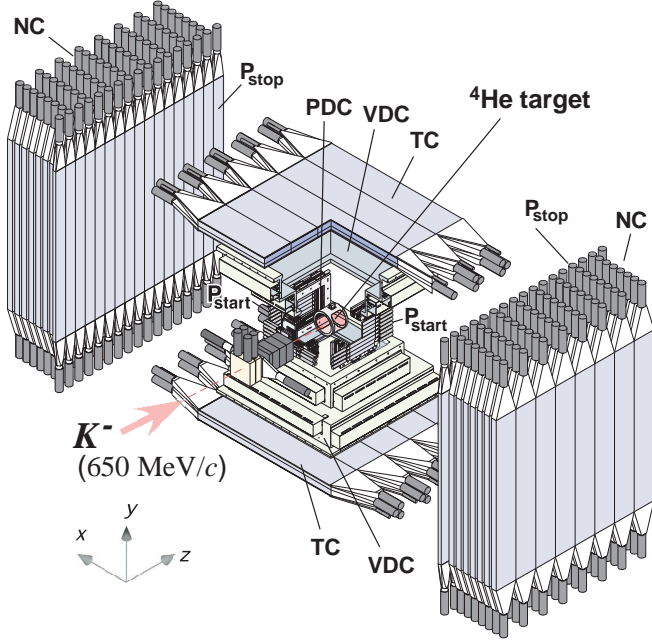


**Fig. 1.** Present experimental setup. The setup is constructed symmetrically around the central liquid helium target. Left and right arm are neutron counter arrays (NC). In front of NC, new segmented proton TOF stop counters were installed. These horizontal counters are used to achieve the proton inclusive spectroscopy. Top and bottom counters are primarily for the decay charged particle  $X^\pm$  detection, which is indispensable for the neutron spectroscopy or the detailed analysis using decay particles.

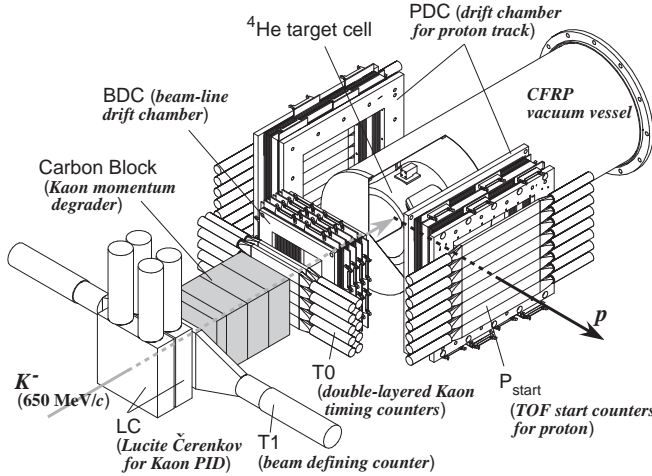


**Fig. 2.** Close up view of the experimental setup around the target region. Segmented proton TOF start counter arrays are placed behind the proton tracking chambers (PDC). The segmented neutron TOF start counters (T0), placed in front of the beam kaon tracking chamber (BDC), were upgraded to the double layered structure to achieve better resolution of the neutron TOF analysis.

On the other hand, proton TOF can be performed more directly with dedicated start and stop counters and the proton track information itself. Therefore, we newly installed drift chambers (PDC) and fine segmented start- ( $P_{\text{start}}$ ) and stop- ( $P_{\text{stop}}$ ) counters for proton spectroscopy as shown in Fig. 2. We removed thin charged-veto counters and iron plates in front of the NC array, instead, to enlarge the acceptance for low momentum protons. With this setup, we can perform inclusive proton spectroscopy of the  ${}^4\text{He}(\text{stopped } K^-, p)$  reaction over a wide momentum range without requiring an additional  $X^\pm$  track on TC. The statistics of the inclusive proton spectrum can be significantly improved compared to the previous semi-inclusive proton spectrum of the  ${}^4\text{He}(\text{stopped } K^-, pX^\pm)$  reaction, whose statistics were limited by the solid angle of TC. In the present analysis, we can also check the consistency of our momentum analysis procedure using redundant information of proton TOF between T0,  $P_{\text{start}}$  and  $P_{\text{stop}}$  counters.

We also improved particle identification (PID) capability of the TC counters for  $X^\pm$  by adding additional two layers to the previous *E471* setup (namely 2+2 layers), because high momentum protons above  $\sim 500$  MeV/ $c$  cannot be separated from pions in the *E471*. The PID analysis on TC shows that we can discriminate pions from protons over a wide momentum range from 300  $\sim$  600 MeV/ $c$ , so that we can reconstruct the hyperon invariant mass using  $\pi N$ -pairs detected in TC and NC.

We performed two experiments *E549/E570* at KEK both aimed at confirmation of the  $S^0(3115)$  in the improved proton spectrum, and obtaining higher neutron statistics for a detailed study together with the other decay products. *E549* is the dedicated experiment for  ${}^4\text{He}(\text{stopped } K^-, N)$  spectroscopy. We also accumulated data parasitically in *E570*, whose primary object is the precise measurement of the  $3d \rightarrow 2p$  x-ray energy in kaonic helium atoms. By using roughly seven times the beam time compared to *E471*, we accumulated about 50 times more statistics for proton inclusive data and 10 times more for neutron. In the case of neutron analysis, we do need  $X^\pm$  recorded on TC as in the previous experiment, so that the statistics improvement comes mainly from the larger NC counter volume.

After the slewing correction, to compensate the time-walk caused by the finite discriminator threshold, the TOF resolution (RMS) was improved from 300  $\rightarrow$  120 psec for protons and 300  $\rightarrow$  200 psec for neutrons. The difference of time resolution improvements comes from the TOF definition between the two. For proton TOF between  $P_{\text{start}}$  and  $P_{\text{stop}}$ , the slewing function is calibrated by using  $K\mu\text{II}$  and  $K\pi\text{II}$  decay events from  $K^+$  runs. Neutron TOF is measured between T0 and the NC array, instead, and it is calibrated using  $\gamma$ -ray events in  $K^-$  runs.

### 3 Proton spectra

The primary object of the upgraded experiment at KEK is to confirm whether or not the previous interpretation of the  $S^0(3115)$  peak formation in the proton spectrum

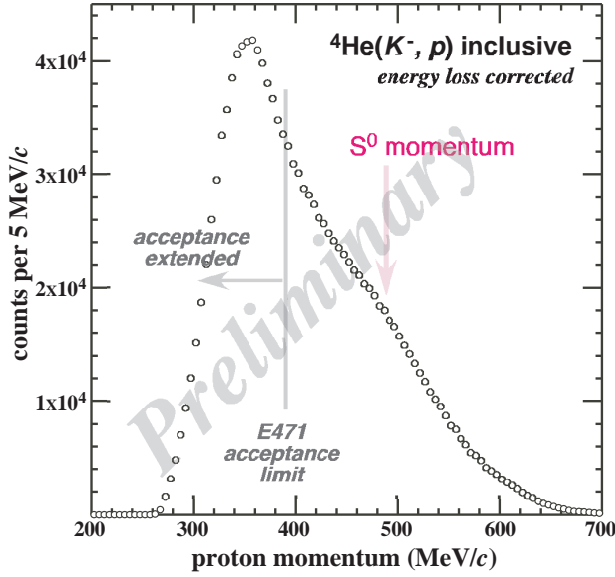


**Fig. 3.** Inclusive proton momentum spectrum. The proton TOF is measured by the time difference between  $P_{\text{start}}$  and  $P_{\text{stop}}$  counters.

is true. Let us focus on the proton spectroscopy in this paper, because the neutron spectroscopy will be given in another paper [3].

The inclusive  ${}^4\text{He}(\text{stopped } K^-, p)$  proton TOF spectrum between  $P_{\text{start}}$  and  $P_{\text{stop}}$  counters with PDC tracking information is shown in Fig. 3. The proton PID on NC counters is performed by using the correlation between  $1/\beta$  and total energy deposit in the  $P_{\text{stop}}$  and the NC array. The initial proton momentum was computed iteratively using energy-loss calculation code, so as to obtain consistent  $P_{\text{start}}$  and  $P_{\text{stop}}$  timing by assuming that the proton is originated from the primary kaon reaction point given by the vertex determined from kaon and proton tracks. Because of target,  $P_{\text{start}}$ , and the air, the momentum differed from simple TOF calculation by about 30 MeV/c. The error of the momentum caused by the analysis procedure is small enough compared to the time resolution, except for the proton caused by the hyperon decay.

The spectrum is much different from that of the previous *E471* experiment [1], i) the statistics are drastically improved, ii) the proton momentum acceptance is extended to the low momentum side substantially, and iii) there is no clear peak structure at the momentum where we expected the signal from  $S^0(3115)$  formation.

Why does the signal disappear in the inclusive proton spectrum? It is extremely important to examine the  ${}^4\text{He}(\text{stopped } K^-, pX^\pm)$  spectra. Most significantly, the peak was seen clearly in the charged-pion-tagged spectrum, but it was not in the proton tagged one in *E471*. If the  $S^0(3115)$  peak formation was due to the simple experimental defect, it would be seen in both spectra.

Figure 4 shows the  ${}^4\text{He}(\text{stopped } K^-, pX^\pm)$  spectra. The statistics of both are substantially reduced due to the solid angle of TC. The decay particles  $X^\pm$  on TC are re-

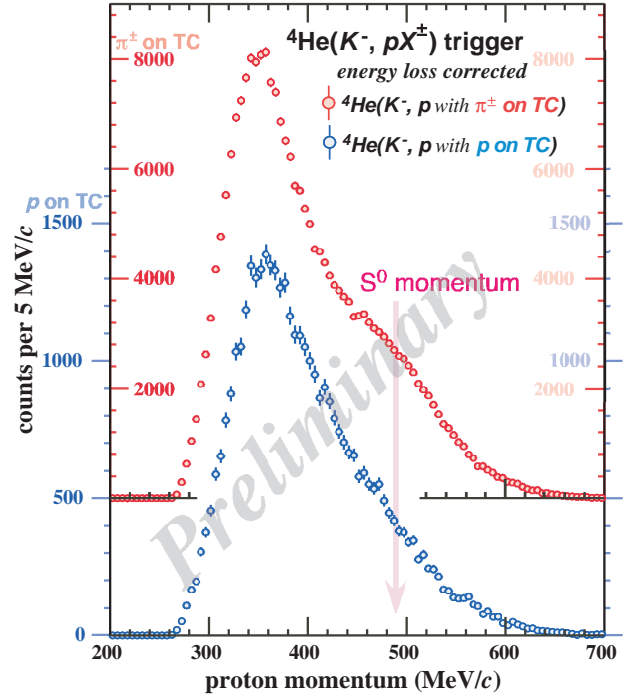


**Fig. 4.** Proton momentum spectra of  ${}^4\text{He}(\text{stopped } K^-, pX^\pm)$  reaction. Spectra of charged pion (right-scale) and proton (left-scale) tagged on TC are shown separately. These spectra are the subset of Fig. 3. Note that the vertical scales are different between the two.

quired in the software level to reproduce the *E471* trigger condition, although peak formation is seen in neither of the proton spectra. Therefore, the result is not consistent with *E471*.

Note also the spectral difference between the two at momentum over 400 MeV/c. A rounded elevation is seen in the charged-pion tagged spectrum, while a monotonic decrease results from proton tags. Before discussing the spectral difference, let us focus on the reason why a narrow peak,  $S^0(3115)$ , was seen in the *E471* proton spectra.

#### 4 Difference of the proton TOF analysis

It is crucial to understand why and how the results are inconsistent to each other. The present data indicates that some of the previous analysis procedure might give a spectral-singularity slightly below 500 MeV/c in the proton spectra.

Actually, this is the momentum where a proton stops at the back side of the proton TOF stop counter in *E471* (NC first layer in that setup). Therefore, we performed Monte Carlo simulations to study the light-output response of the NC first layer as a function of the original proton momentum at the reaction point assuming the configuration of the previous *E471* experimental setup.

Figure 5 is the result of the simulation, where the horizontal axis is the proton initial momentum and the vertical axis is the expected light output from the plastic scintillator with the thickness of 5 cm. In the simulation, reaction

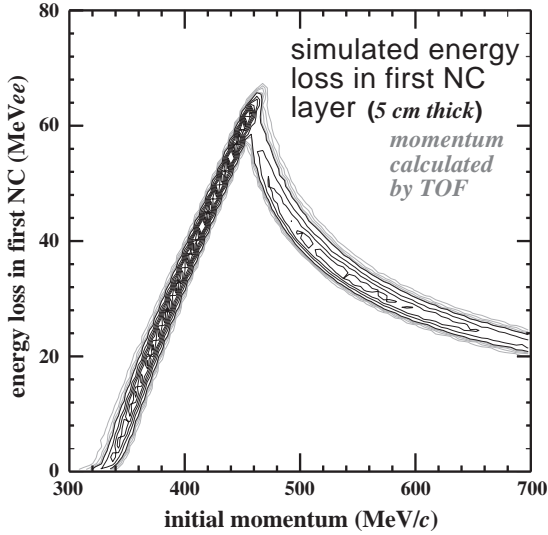


**Fig. 5.** Contour plot of the simulated energy loss in the proton TOF stop counter (NC first layer as for the *E471* experimental configuration whose thickness is 5 cm). The light saturation at high  $dE/dx$  (Birk's effect) is taken into account.

point distribution and the counter resolution (light collection efficiency to the PMTs at both ends) are taken into account, which makes the distribution band width to be wider.

The light output distribution in the counter has cusp-like structure at around 460 MeV/ $c$ . The lower momentum side gives less light output, because the range is shorter than the counter thickness. The protons whose momentum below 320 MeV/ $c$  never reach the TOF stop counter. The light gets smaller again on the higher momentum side as they approach minimum ionizing particles (MIPS)  $\sim 10$  MeVee (electron equivalent) in 5 cm thick plastic counter. The sudden drop of the light output is due to the nature of the Bragg curve, which has maximum energy loss before the charged particle stops.

This cusp-like singularity may cause a severe problem in the TOF analysis procedure. As it is described, TOF start and stop counters hit-time information is corrected so as to have best resolution for MIPS ( $K\mu\text{II}$  events). The typical slewing correction function is written as:

$$t = \frac{T_A + T_B}{2} - \left( \frac{c_A}{\sqrt{A_A}} + \frac{c_B}{\sqrt{A_B}} \right) - T_0, \quad (1)$$

where  $T_A$  and  $T_B$  are the TDC data of the PMT at both ends of a counter,  $A_A$  and  $A_B$  are that for charge sensitive ADC for the signal pulse,  $c_A$  and  $c_B$  are the correction parameters, and  $T_0$  is time-offset of the counter. The parameters  $c_A$ ,  $c_B$  and  $T_0$  were defined and calibrated for each counter to minimize the  $1/\beta$  ( $= c\Delta t/\Delta L$ ) distribution width at known  $1/\beta$  value for the MIPS.

The problem is that the correction formula (1) depends on the energy deposit in the counter. The typical energy deposit in the cusp region is  $\sim 6$  times higher in energy than that of MIPS (calibration point) so that the simple

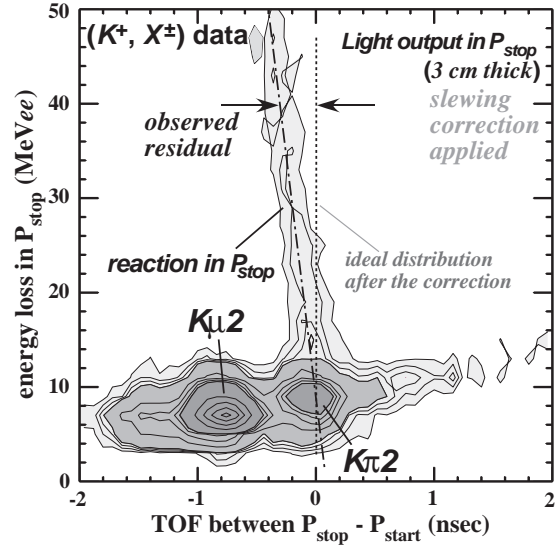


**Fig. 6.** Energy loss observed in  $P_{\text{stop}}$  (3 cm thick) counter for  $(K^+, X^\pm)$  events obtained in *E549*. Simple slewing correction defined by MIPS has been applied. The horizontal axis is the TOF between  $P_{\text{start}}$  and  $P_{\text{stop}}$ , and the vertical axis is the light output of  $P_{\text{stop}}$  counter.

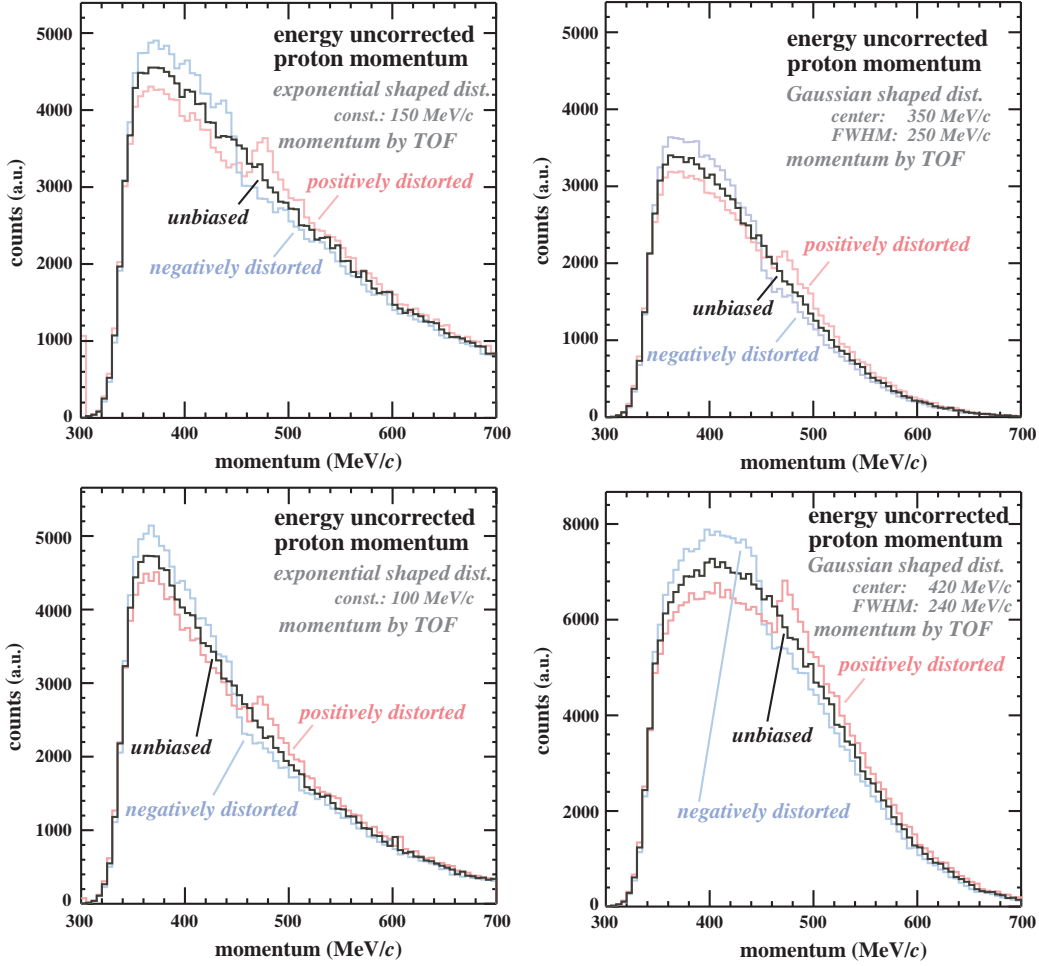
application of the formula may result in a deformation of the TOF spectrum at around 460 MeV/ $c$ .

Figure 6 is a contour plot of  $1/\beta$  and energy deposit in the TOF stop counter ( $P_{\text{stop}}$ ) of *E549*. The horizontal axis is the  $1/\beta$  obtained from  $P_{\text{start}}$  and  $P_{\text{stop}}$  counters after the simple slewing correction (1) has been applied. The vertical axis is the position-averaged light output of the  $P_{\text{stop}}$  counter in the form of  $\sqrt{A_A A_B}$  ( $= \bar{A}$ ) to cancel the light attenuation effect in the first order. In the figure, a higher energy component is seen originating from the  $K\pi\text{II}$  peak. The light output of these events in the  $P_{\text{start}}$  counter is consistent with MIPS, so that the large energy observed in the  $P_{\text{stop}}$  counter should be the result of nuclear reaction of the pion in  $P_{\text{stop}}$ .

If the slewing correction function (1) is applicable to the large energy deposit region, no correlation is expected in this figure. However, the pion reaction events are inclined towards upper-left of this figure. It clearly indicates that the slewing correction by the formula (1) is not sufficient, and most of the counters have similar residuals as a function of energy deposit in the counter. In the previous *E471* experiment, the TOF calibration was performed using  $\gamma$ -ray events. The  $\gamma$ -ray was converted to the electron shower at the iron plate located in between the NC array and the thin charged-veto counters (removed from the present setup). Very unfortunately, the  $\gamma$ -ray originated signals don't give large energy deposit in the TOF stop counter. Therefore, there is no good calibration data at the high energy deposit region.

The simplest term to cancel the residual correlation between time and pulse-height can be written as:

$$\Delta t = c_R (\bar{A} - A_0), \quad (2)$$



**Fig. 7.** Simulated distortion effect due to the residual time versus pulse-height of the proton TOF spectra. Upper left and lower left panels are the result of exponential proton spectra with the constant of 150 and 100 MeV/c, respectively. Upper right and lower right ones are for Gaussian distribution center and width of 350 and 250 (upper), and 420 and 240 MeV/c (lower), respectively. TOF linear distortion of  $\pm 5$  psec/MeVee is assumed for all the spectra. The momentum loss of the proton is not corrected.

where  $A_0$  is the average ADC count for MIPS. In the case of  $E549/E570$  data, a more precise correlation function could be defined for each counter, though the formula (2) is enough to simulate what may happen in the previous  $E471$  analysis.

The effect of the hidden-residual term in the proton TOF analysis to the proton momentum spectrum can be reproduced by intentionally adding the residual to the simulated one. We have performed the simulations by assuming several artificial proton spectra with the deformation parameter  $c_R$  as small as  $\pm 5$  psec/MeVee.

As shown in the figures, all the spectra have distortion slightly above the cusp region where  $S^0(3115)$  was found in  $E471$  analysis, when the TOF is distorted in the positive direction. The peak structure is more clearly seen when the original proton spectrum has rounded elevation around the momentum (lower-right panel of the figures). This is consistent with the result of  $E471$  analysis that the  $S^0$  is seen more clearly in the pion tagged distribution, which have rounded elevation around the momentum.

Therefore, it is concluded that the  $S^0(3115)$  peak observed in proton spectrum in  $E471$  is most likely formed as an experimental artifact, when the range of the particle matches to the counter thickness. On the other hand, such artificial peak formation cannot be expected in the neutron spectrum, because the neutron can be detected at any depth of the NC counter.

## 5 Upper limit of the peak formation

In the present experiment, one of the important questions to be answered is what is the upper limit of formation of the kaonic nuclear bound state from the inclusive proton spectrum.

To obtain the upper limit of the formation of kaonic nucleus per kaon reaction at rest, we need to evaluate the number of the stopped kaon in the helium target and proton acceptance as a function of its momentum. We evaluated the number using the known free decay branch of

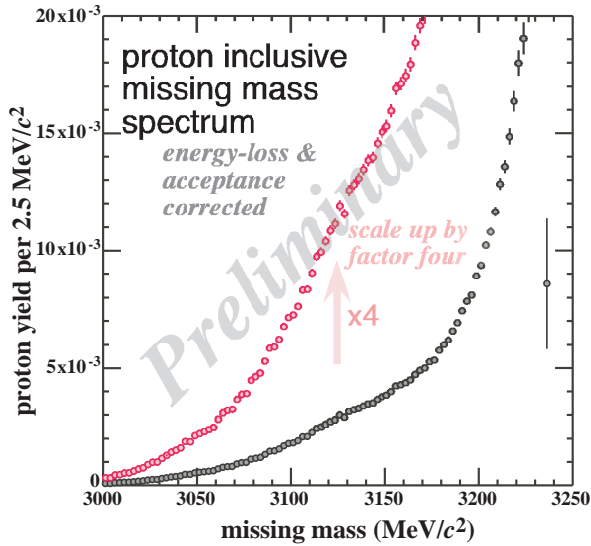


Fig. 8. Acceptance corrected proton missing mass spectrum.

so called meta-stable kaons  $3.5 \pm 0.5\%$  [4] (a negative kaon in the atomic orbit of helium at a large angular momentum). The proton detection efficiency has momentum dependence, because of the range at the low momentum side and the proton PID at the high momentum side. We identified the proton using its momentum and total energy recorded in the NC array. The higher momentum side of the proton spectrum given in Fig. 3 has less efficiency compared to the low momentum side, due to the reduction of the effective solid angle and reaction loss of the proton. The proton detection efficiency is calculated by a simulation.

Figure 8 shows the missing mass spectrum of protons after the acceptance correction. In this figure, the vertical axis is normalized by the number of stopped kaons. We have evaluated the upper limit by assuming a smooth proton spectral function (third polynomial function) together with a Gaussian centered at  $3115 \text{ MeV}/c^2$ . The upper limit of the narrow ( $\Gamma < 20 \text{ MeV}/c^2$ ) peak formation at this mass region is obtained to be well below  $10^{-3}$  at the 95% confidence level. This upper limit is quite severe compared to the at-rest kaon-induced hypernuclear formation probability of the order of %. Therefore, the existence of such a narrow state is not very likely.

## 6 Discussion and Conclusion

As it is described, the signal of  $S^0(3115)$  observed in  $E471$  is most likely due to the experimental artifact. This experimental problem exist only in proton, but not neutron spectroscopy. The upper limit of the formation probability of such a narrow peak ( $\Gamma < 20 \text{ MeV}/c^2$ ) is in the order of  $10^{-4}$  at  $S^0$  energy. However, it does not exclude the existence of a wider structure.

The sensitivity for the wider structure is limited because of the large background, so that it is very important to understand background components of the proton spectrum.

The dominant reaction branch of the kaon reaction at rest is known to be quasi-free hyperon production with pion emission, namely  $K^-N \rightarrow Y\pi$ . If this is the primary reaction, then most of the energy is carried out by the pion kinetic energy, so that the proton (or nucleon in general) from the hyperon decay is dominantly produced at momenta lower than  $\sim 400 \text{ MeV}/c$  (cf. Fig. 4) or above  $\sim 3200 \text{ MeV}/c^2$  in the missing mass spectrum (cf. Fig. 8). The nucleons produced by  $\Sigma$ - $\Lambda$  conversion,  $\Sigma N \rightarrow \Lambda N$ , are also located mostly in the same region. It is difficult to improve sensitivity to detect wider structures in this region, because the spectrum changes drastically depending on the momentum.

On the other hand, the higher momentum region above  $\sim 400 \text{ MeV}/c$  is more simple. This region originates dominantly from non-mesonic kaon absorption,  $K^-NN \rightarrow YN$ . Actually, the spectral difference between charged pion and proton tagged spectra shown in Fig. 4 is due to the sensitivity to the non-mesonic process. This is because of the kinematics of the hyperon decay,  $Y \rightarrow N\pi$ . The direction of  $Y$  and  $N$  is almost the same in the Lab. frame while the  $\pi$  distribute almost uniformly, because of the small pion mass. Therefore, the pion tagged one is more sensitive to the non-mesonic kaon absorption process, which gives rounded elevation of the spectrum at high momentum region.

In the  $E471$  analysis, improvement of the signal-to-noise ratio in this momentum region was intended using pion-trajectory defined hyperon motion [5]. The original idea of the analysis is to try to improve the signal fraction by selecting low momentum hyperon in the final state. The  $Q$ -value of the background  $K^-NN \rightarrow YN$  (non-mesonic) process is very large, so that the kinetic energy of the hyperon is expected to be larger than that of signal. Actually, same analysis as reference [5] gives similar spectral enhancement of broad structure in neutron spectra, but we need to study the data more carefully, because the kinematical difference between the signal and non-mesonic is not extremely large, and the difference becomes more marginal if final state interaction of the hyperon is taken into account.

With the present higher statistics data, we are presently analyzing data based on the invariant mass similar to the FINUDA paper [6]. The analysis is in progress and the result will be reported in the near future.

## References

1. T. Suzuki et al., Phys. Lett. B **597**, (2004) 263.
2. Y. Akaishi and T. Yamazaki, Phys. Rev. C **65**, (2002) 044005.
3. H. Yim et al., Proceedings of HYP06, Johannes Gutenberg University Mainz.
4. T. Yamazaki et al., Phys. Rev. Lett. **63**, (1989) 1590, H. Oota Doctoral Dissertaion, Univ. of Tokyo (2003).
5. M. Iwasaki et al., arXiv: nucl-ex/0310018.
6. M. Agnello et al., Phys. Rev. Lett. **94**, (2005) 212303.

